

On the elimination of refractive-index variations in turbulent density-stratified liquid flows

By TREVOR J. McDOUGALL

Research School of Earth Sciences, Australian National University,
P.O. Box 4, Canberra 2600

(Received 2 February 1978 and in revised form 3 November 1978)

The variations in refractive index in stratified liquid flows have been a major impediment to the use of laser-Doppler anemometry in these situations. This paper describes a method whereby these refractive-index variations can be drastically reduced while retaining the dynamically important density differences. The method uses two solutes to produce the density differences and it is shown that double-diffusive convection (of the salt-finger type) can be avoided by using a suitable pair of solutes. A theoretical model of the lateral wander of a single laser beam propagating through a turbulent medium is developed and this explains the success of the method.

1. Introduction

A laser-Doppler anemometer has two laser beams which cross at the point in the fluid where measurements are required. The small region of intersection of the laser beams is called the probe volume (or measurement control volume). One velocity component of small particles which pass through the probe volume is determined from the Doppler frequency of the light which is scattered by the particles within this probe volume. When a laser-Doppler anemometer is used in a turbulent flow with refractive-index variations, the laser beams do not remain stationary in space, and if the variations in refractive index are not small, the laser beams cross only intermittently. This causes a severe loss of signal (called 'drop-out'). Even when the laser beams do intersect to form a probe volume, the signal received by the anemometer has a random superimposed velocity shift due to the relative velocities of the laser beams.

A method has been developed whereby the refractive indices of two solutions can be made very nearly equal, while retaining a density difference between the solutions. This enables the use of laser-Doppler anemometry in a whole range of experiments involving turbulence and mixing in stratified liquids. In these flows, the buoyancy forces caused by differences in density are often all-important in determining the fluid motions. A general reference for these types of flow is Turner (1973).

The method relies on the fact that various solutes in, say, water can contribute to the density and to the refractive index of the solution in different proportions. The problem of double-diffusive convection needs to be circumvented, and Huppert & Manins (1973) have derived a condition (for the salt-finger regime) under which this phenomenon is avoided. This criterion further restricts the choice of suitable pairs of solutes.

In the experiments reported herein, Epsom salts and sugar have been used as the two solutes. The refractive index of a solution of two solutes is often approximated by the first few terms of a Taylor series in the two concentrations, and in this paper we consider in detail the influence of terms up to second order.

The limitations on the matching of the refractive index of all parts of a stratified turbulent flow are due to (i) the accuracy of measurement of the refractive index of the two original solutions, (ii) the nonlinearity of the refractive index as a function of the concentrations of the solutes and (iii) the different molecular diffusivities of the solutes, which cause a slight mismatch of the refractive index when molecular diffusion is important, for example at a density interface. This slight mismatch due to diffusion does not increase in magnitude but it spreads out as the square root of time (like any slow diffusion process).

In §6 a theory is developed to quantify the lateral wander of a single laser beam as it propagates through a fully turbulent medium.

It is perhaps worth mentioning that the idea of matching refractive indices is not new. Carlos & Richardson (1967) studied the motion of fluid around glass spheres by using a fluid which had the same refractive index as glass. Recent laser-Doppler measurements of the flow around banks of cylinders have been made possible by using Pyrex cylinders and a fluid mixture of 95% trichloroethylene and 5% acetone. The method of this paper is essentially very different because it is concerned with *miscible, stratified* liquids.

2. Requirements of the solutes

Let us consider two solutes A and B dissolved in a solvent, say water. The diffusivities will be denoted by κ_A and κ_B , and we restrict our attention to the case where the solute of higher diffusivity (which we shall call solute A) is stably stratified and solute B is unstably stratified. This is the regime in which we may expect salt fingering to occur.

We want to avoid the occurrence of salt fingers because we wish to be able to study the fluid motions associated with turbulence, and we do not want these motions to be complicated by the presence of double-diffusive convection.

The refractive index n and the density ρ of a solution (at 20 °C) of both A and B can be expressed by the Taylor series

$$n = 1.3330 + a_n C_A + b_n C_B + \text{higher-order terms}, \quad (1)$$

$$\rho = 0.9982 + a_\rho C_A + b_\rho C_B + \text{higher-order terms} \quad (\text{g/ml}), \quad (2)$$

where C_A is the concentration of component A in units of (weight of solute per unit weight of solution). It is advantageous to use this definition of C_A (as opposed to, say, weight of solute per unit volume of solution) as the total weight of the solutions and the weights of each solute are strictly additive quantities when the mixing together of two solutions is considered. We initially consider only the first-order (linear) terms in (1) and (2). In a later section we consider the effect of the second-order terms as well.

Consider a two-layer system in which a more dense solution 1 lies below a less dense solution 2. Note that now, in accordance with our initial assumptions, we must

have $C_{A1} > C_{A2}$ and $C_{B2} > C_{B1}$, where C_{A1} is the concentration (in g/g of solution) of solute A in solution 1 etc. The restriction that the refractive indices be equal (i.e. $n_1 = n_2$) then reduces to [from (1)]

$$a_n(C_{A1} - C_{A2}) = b_n(C_{B2} - C_{B1}). \quad (3)$$

Let τ be the ratio of the diffusivities, $\tau = \kappa_B/\kappa_A$ (< 1), and let the density-anomaly ratio R_ρ^* be defined by $R_\rho^* = a_\rho(C_{A1} - C_{A2})/b_\rho(C_{B2} - C_{B1})$, where $a_\rho(C_{A1} - C_{A2})$ and $b_\rho(C_{B2} - C_{B1})$ are the differences between the densities of solutions 1 and 2 due to solute A or B alone (respectively). Note that the two-layer fluid system is gravitationally statically stable if $R_\rho^* > 1$. Huppert & Manins (1973) have shown that if

$$R_\rho^* > \tau^{-\frac{1}{2}} \quad (4)$$

salt fingers are not able to form at the horizontal interface between the two solutions, even though the other requirements for salt fingers are fulfilled. In order to avoid salt fingering while having equal refractive indices, we need [from (3) and (4)]

$$\frac{a_n}{a_\rho} \kappa_A^{\frac{3}{2}} < \frac{b_n}{b_\rho} \kappa_B^{\frac{3}{2}}. \quad (5)$$

This equation is the essential constraint on the parameters a_ρ , b_ρ , a_n , b_n , κ_A and κ_B of the solutes A and B .

The analysis of Huppert & Manins is for the possibility of the development of steady regular salt fingers on a flat horizontal interface, but we expect that salt fingers will not be able to grow at, say, the edge of a turbulent eddy if inequality (5) is satisfied by a large enough margin. This expectation was confirmed by the experiments, as no salt fingers were observed.

In the type of experiment for which this method is intended, one will normally wish to have a known density difference between two solutions and the flow will mix the solutions with each other in a turbulent manner. The difference in the diffusivities between the solutes will try to distribute the solutes unevenly (by the process of molecular diffusion), but if the time scale involved in the turbulent process is small (so that molecular diffusion is not given much time to be effective), then we may regard the working fluid (at any location and time) as being composed of a linear combination (by mixing) of the two original solutions. If the linear equation (1) were exact, and if we had the refractive indices of the two solutions equal initially, then the refractive index of a mixed linear combination of the two solutions would be unchanged.

The most convenient pair of solutes for use in the laboratory was found to be Epsom salts and sugar. These are both relatively cheap and readily available. The constants for these solutes are (solute A is Epsom salts) $\kappa_A = 0.61 \times 10^{-5} \text{ cm}^2 \text{ s}^{-1}$, $a_n = 0.20286$, $a_\rho = 1.0054 \text{ g/ml}$, $\kappa_B = 0.45 \times 10^{-5} \text{ cm}^2 \text{ s}^{-1}$, $b_n = 0.14445$ and $b_\rho = 0.38407 \text{ g/ml}$, giving $\tau = 0.738$ and $\tau^{\frac{1}{2}} = 0.633$. Inequality (5) is satisfied with the right-hand side 18% greater than the left-hand side. The values of the diffusivities were taken from Huppert & Manins (1973) and the other constants were found by a least-squares fit to the data in Weast (1971) (see below).

3. Effects of deviation from linearity of the refractive-index expression

When two solutions of the same refractive index are mixed together, the resulting solution has a refractive index close to but not exactly equal to that of the original solutions. This behaviour is to be expected because of the nonlinear terms in (1) and it is necessary to quantify this effect in order to know how much the refractive index will vary in a turbulent mixing environment.

The refractive index of a solution (at 20 °C) of both Epsom salts and sugar can be expressed more accurately as

$$n = 1.3330 + 0.20286C_A - 0.0061C_A^2 + 0.14445C_B + 0.043C_B^2 + 0.158C_AC_B. \quad (6)$$

Shirtcliffe (1973) has found that a similar expression describes the behaviour of a sugar-salt solution rather well, although his concentrations were expressed in terms of the (less convenient) mass of solute per unit *volume* of solution. The values of the coefficients in (6) (except for the last one) were found by a least-squares fit to the data tabulated in Weast (1971) for the two cases $C_A = 0$ and $C_B = 0$. The coefficient of the cross-term (0.158) was estimated as follows. A solution of Epsom salts and a solution of sugar with known refractive indices and hence known C_A and C_B (equal to 0.14507 and 0.14590 respectively) were prepared. These were then mixed in varying proportions and the refractive index measured. Five measurements were made and the value of the coefficient was estimated as 0.158 ± 0.006 , where the error limits represent the maximum experimental error. Equation (6) is then expected to be accurate to within ± 0.0001 in the range $0 < C_A < 0.15$ and $0 < C_B < 0.15$.

We are now in a position to determine how the refractive index of a mixture of an Epsom-salts solution (say solution 1 with $C_{B1} = 0$ and Epsom-salts concentration equal to C_{A1}) and a sugar solution (say solution 2 with $C_{A2} = 0$ and sugar concentration equal to C_{B2}) varies with the mixture ratio m , defined by

$$m = \frac{\text{weight of sugar solution}}{\text{total weight of the mixed solution}}. \quad (7)$$

The resultant C_A and C_B of the mixture are then given by

$$C_A = (1 - m)C_{A1}, \quad C_B = mC_{B2}, \quad (8)$$

so

$$n = 1.3330 + 0.20286(1 - m)C_{A1} - 0.0061(1 - m)^2C_{A1}^2 + 0.14445mC_{B2} + 0.043m^2C_{B2}^2 + 0.158m(1 - m)C_{A1}C_{B2}. \quad (9)$$

We are interested in the situation where the refractive indices of the two original solutions are equal (i.e. $n_1 = n_2$). Figure 1 shows the change in the refractive index of a mixture of the two solutions as a function of m for values of n_1 ranging from 1.3330 to 1.3650 in equal steps of 0.0020. These steps correspond to approximately equal steps in the density difference between the solutions of 0.0048 g/ml. For each value of $n_1 (= n_2)$ the largest deviation of n from n_1 is the value of n at $m = 0.5$ (i.e. $dn/dm = 0$ at $m = 0.5$ for all n_1). This maximum value of $n - n_1$ can be read from figure 1 at $m = 0.5$, and is also shown more clearly on figure 2 as a function of n_1 .

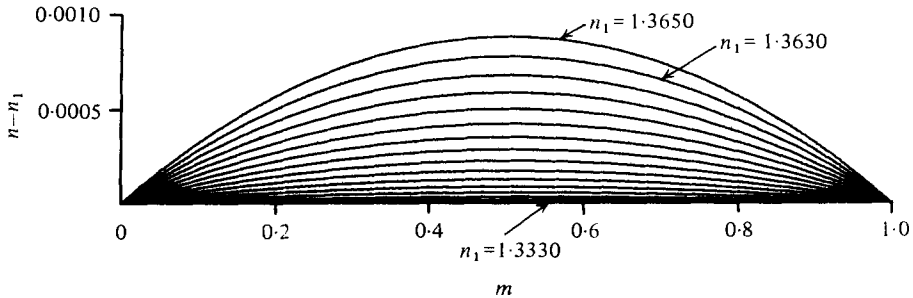


FIGURE 1. The deviation in the refractive index from n_1 when two solutions of equal refractive index are mixed in the mixture ratio m . One solution (called solution 1) is an Epsom-salts solution and the other solution (solution 2) is a sugar solution. The curves are for values of n_1 ranging from 1.3330 to 1.3650 in steps of 0.0020.

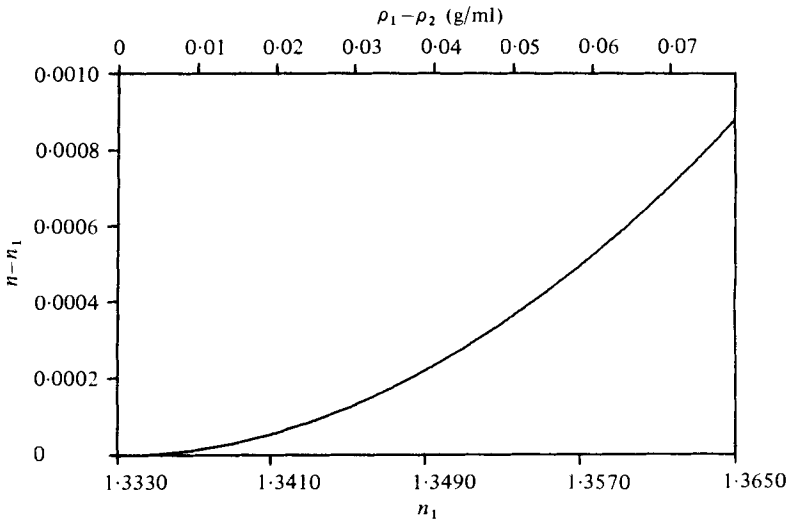


FIGURE 2. Graph of the maximum deviation of n from n_1 as a function of n_1 for the curves on figure 1. The density difference between the two solutions ($\rho_1 - \rho_2$) is also shown as an alternative abscissa.

In some flows which are driven by a density difference there are significant regions of the flow where the mixture ratio m does not vary very much from some average value m_0 . It is beneficial to have $dn/dm = 0$ at $m = m_0$ in this situation, on which case small variations in m about m_0 produce only second-order variations in the refractive index. The case $m_0 = 0.5$ is depicted in figure 1 (where $n_1 = n_2$). It is easy to arrange that $dn/dm = 0$ at any desired m_0 simply by choosing n_2 to be slightly different from n_1 . Differentiating (9) with respect to m and setting it equal to zero at $m = m_0$, we obtain

$$0.086 m_0 C_{B2}^2 + C_{B2} \{0.14445 + 0.158 C_{A1} (1 - 2m_0)\} - 0.20286 C_{A1} + 0.0122 (1 - m_0) C_{A1}^2 = 0. \quad (10)$$

For a given n_1 (i.e. given C_{A1}) this equation is readily solved for C_{B2} (and hence n_2) in terms of the desired m_0 . Figure 3 shows $n_2 - n_1$ as a function of m_0 for various values

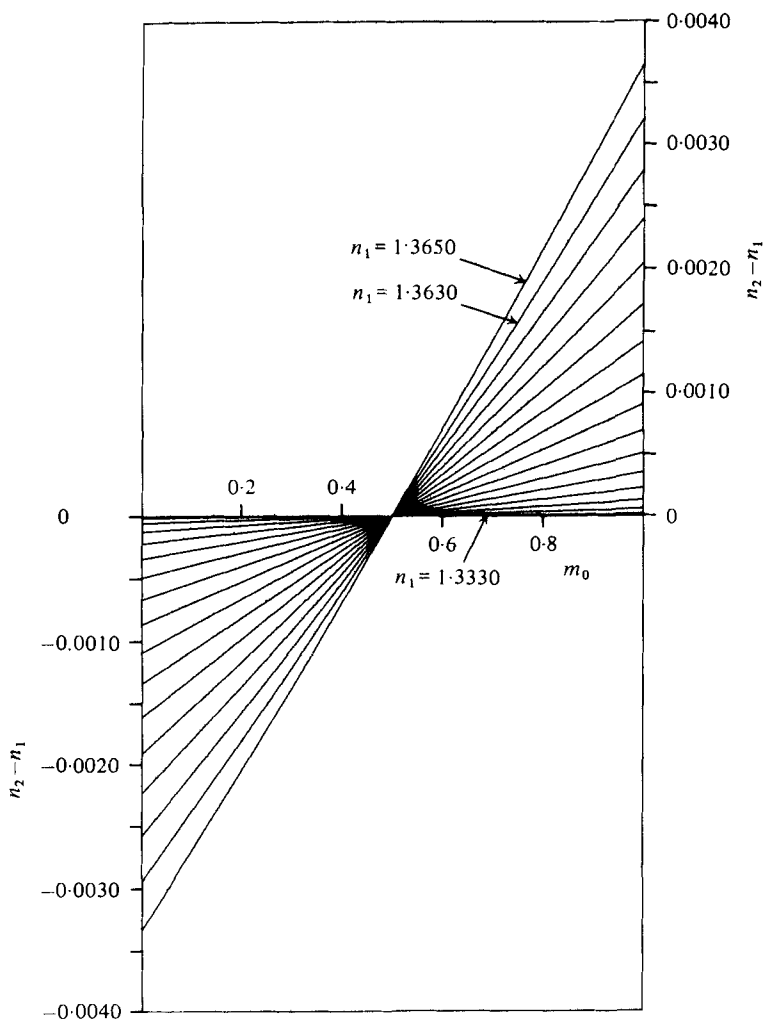


FIGURE 3. Graphs of value of $n_2 - n_1$ required to ensure that dn/dm is zero at m_0 , plotted as a function of m_0 for various values of n_1 .

of n_1 . Note that at $m_0 = 0.50$, n_2 is equal to n_1 for all n_1 , which is the case we have considered above.

Having chosen n_1 and m_0 , and then made solution 2 have the refractive index n_2 given by figure 3, we can plot $n - n_1$ as a function of the actual mixture ratio m . Figure 4 shows the two cases $m_0 = 0.25$ and $m_0 = 0.75$.

A realistic measure of the effect of refractive-index variations on the laser beams is the difference between the maximum and minimum refractive indices which occur along the length of the beams. If the range of m encountered along the path of the laser beams is small then we can obtain negligible refractive-index variations by ensuring that dn/dm is zero at the mean value of m . If, however, the value of m ranges from zero up to one, then $n_{\max} - n_{\min}$ is minimized by selecting $n_2 = n_1$, or equivalently, by selecting $m_0 = 0.50$.

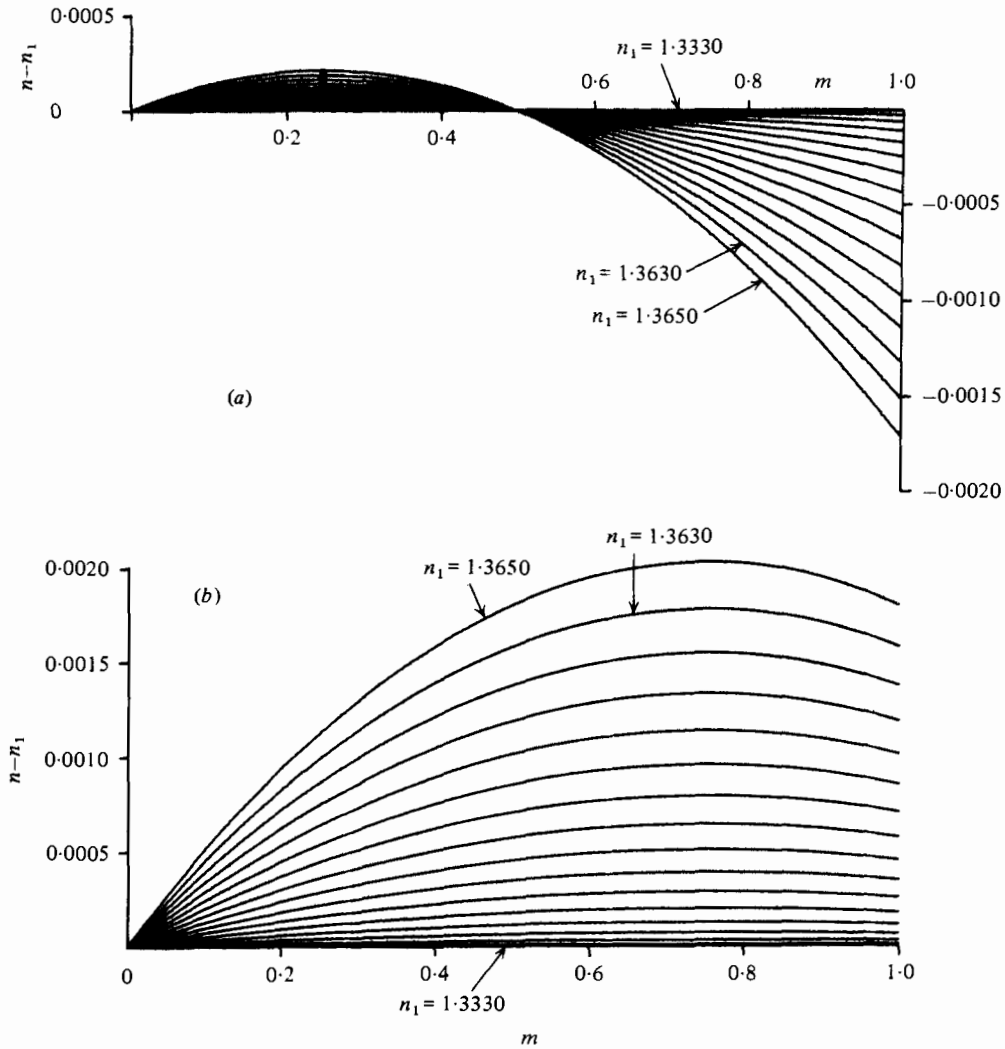


FIGURE 4. Graphs of $n - n_1$ as a function of the mixture ratio m for (a) $m_0 = 0.25$ and (b) $m_0 = 0.75$. The curves are for values of n_1 ranging from 1.3330 to 1.3650 in steps of 0.0020.

4. Effect of molecular diffusion at a density interface

The previous section investigated the effects of nonlinear terms in (1) on the refractive index of a mixture of two solutions. In this section we look at how the different rates of molecular diffusion of the solutes A and B (as determined by κ_A and κ_B) distribute these solutes unevenly, thereby affecting both the refractive index and the density.

Let us investigate the behaviour of an initially sharp horizontal interface between a layer of a solution of solute A and a layer of a solution of solute B . Initially the lower layer has a uniform concentration C_{A1} of solute A and $C_{B1} = 0$, while the upper layer has a uniform concentration C_{B2} of solute B and $C_{A2} = 0$. Both solutes obey a diffusion equation, namely

$$\frac{\partial C_A}{\partial t} = \kappa_A \frac{\partial^2 C_A}{\partial z^2}, \quad \frac{\partial C_B}{\partial t} = \kappa_B \frac{\partial^2 C_B}{\partial z^2}, \quad (11a, b)$$

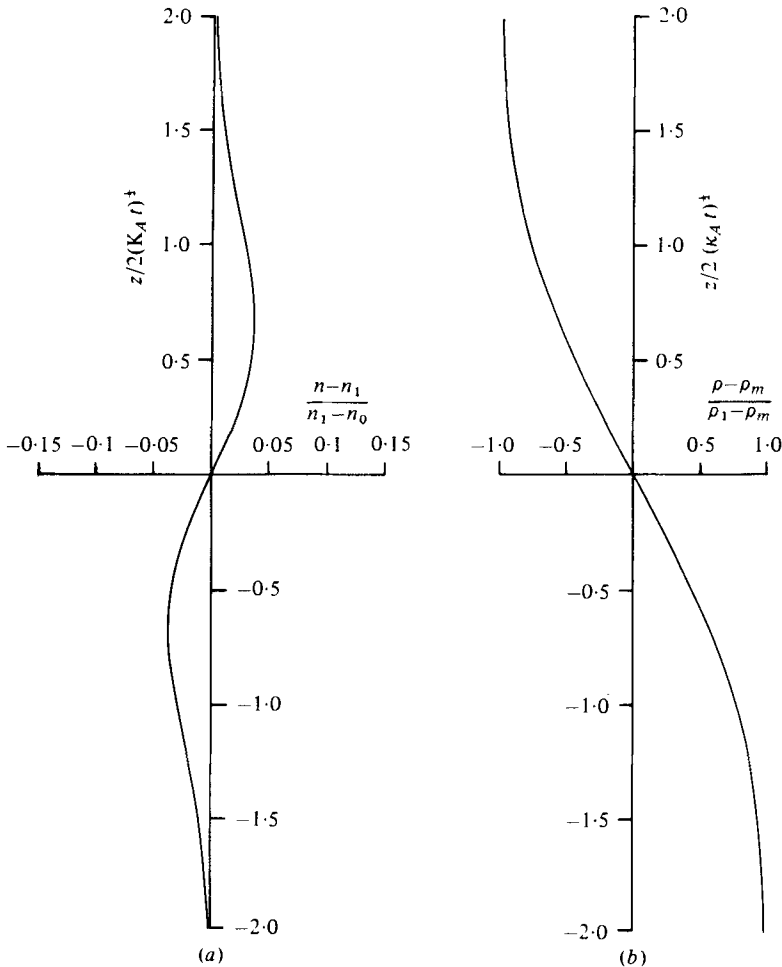


FIGURE 5. Graphs of (a) the refractive index n and (b) the density ρ through a density interface which has been smeared out by molecular diffusion.

and the solutions are readily found to be

$$C_A = \frac{1}{2}C_{A1} \operatorname{erfc}\{z/2(\kappa_A t)^{\frac{1}{2}}\}, \quad C_B = \frac{1}{2}C_{B2} \operatorname{erfc}\{-z/2(\kappa_B t)^{\frac{1}{2}}\}, \quad (12a, b)$$

where z is positive upwards and is zero at the initially sharp interface. We consider the case where the refractive indices of the upper and lower layers are initially equal. Neglecting the nonlinear terms in (1), this means that

$$a_n C_{A1} = b_n C_{B2} = n_1 - n_0 = n_2 - n_0,$$

where n_0 ($= 1.3330$) is the refractive index of fresh water at 20°C . From (1), (2) and (12) we obtain

$$\frac{n(z, t) - n_1}{n_1 - n_0} = \frac{1}{2} \operatorname{erf}\{z/2(\kappa_B t)^{\frac{1}{2}}\} - \frac{1}{2} \operatorname{erf}\{z/2(\kappa_A t)^{\frac{1}{2}}\}, \quad (13)$$

$$\frac{\rho(z, t) - \rho_m}{\rho_1 - \rho_m} = \left[\frac{b_\rho}{b_n} \operatorname{erf}\{z/2(\kappa_B t)^{\frac{1}{2}}\} - \frac{a_\rho}{a_n} \operatorname{erf}\{z/2(\kappa_A t)^{\frac{1}{2}}\} \right] \left(\frac{a_\rho}{a_n} - \frac{b_\rho}{b_n} \right)^{-1}, \quad (14)$$

where $\rho_m = \frac{1}{2}(\rho_1 + \rho_2)$. The values of the constants appropriate to Epsom salts and sugar have been used to plot (13) and (14) and these graphs are shown in figures 5(a) and (b). The important point to note is that the maximum deviation of $n(z, t)$ from n_1 is only 3.6% of $n_1 - n_0$. This maximum occurs at $zt^{-\frac{1}{2}} = \pm 0.00323$ (where z is in cm and t in s) and the profile remains similar at all times. This mismatch of the refractive index will be apparent in practice only at a density interface which exists for quite a long time, such as at the density interface between two well-mixed layers. Measurements with a laser-Doppler anemometer (LDA) have been made through such an interface with the relative density difference across it as high as 1½%. The maximum value of $n(z, t) - n_1$ was equal to $0.036 \times 67 \times 10^{-4} = 2.4 \times 10^{-4}$ in this situation and this was about three times the maximum error that could result from the initial measurement error in setting n_1 equal to n_2 . The interface was just visible on a shadowgraph but no difficulties were encountered with the LDA.

5. Experimental verification of the usefulness of the method

Experiments in stratified liquids often use the shadowgraph technique to observe the liquid motions but when the refractive index is very nearly uniform the shadowgraphs almost completely disappear. Figure 6 (plate 1) shows two shadowgraphs of a forced plume (flow rate about 200 ml/min) of dense liquid emerging from a tube, proceeding without turbulence for a certain distance and then mixing with the liquid of the environment. The density difference between the plume and the surrounding liquid was 0.028 g/ml in both photographs. Figure 6(a) is for a plume of Epsom salts entering a tank of fresh water while figure 6(b) shows a plume of more concentrated Epsom-salts solution entering a tank of sugar solution of the same refractive index (1.34445 ± 0.00005). The plume is clearly visible in figure 6(a) but cannot be seen in figure 6(b). The refractive-index measurements were made with a temperature-compensating hand refractometer (American Optical 10400 TS meter) which can be read to an accuracy of ± 0.00005 . This type of refractometer does not give the *in situ* refractive index, but gives the refractive index that the solution would have at some standard temperature (this is usually an advantage when the instrument is used to measure, say, salinity). An estimate of the effect of a temperature difference on the refractive index of a sugar solution may be gained from the International Critical Tables (Washburn 1927). At worst, the change in refractive index for a temperature difference of 1 °C is only 0.0001, so we conclude that the effect of a temperature difference between the solutions will be negligible if this temperature difference is less than 1 °C.

A single laser beam shining through the turbulent part of the plume moved about by up to 5 mm at the edge of the tank in the case of figure 6(a), but when the refractive indices of the two solutions were matched, no noticeable movement was seen.

A laser-Doppler anemometer, operating in the forward-scatter, fringe mode, was used to estimate the movement of the laser beams. A piece of translucent paper was attached to the side of the tank away from the laser, and the probe volume arranged to coincide with this plane. A rotating diffraction grating provided a frequency shift between the laser beams, and in the absence of any movement of the beams, the photodetector yielded a slightly amplitude-modulated sine wave of this frequency. This small ($\sim 10\%$) amplitude modulation was caused by variations in the transmission

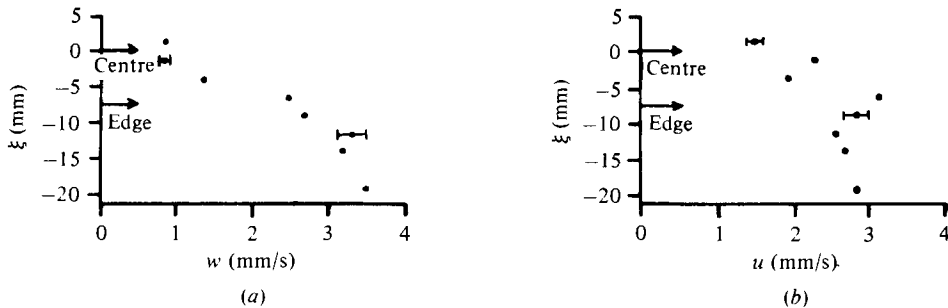


FIGURE 7. Plots of (a) the r.m.s. vertical velocity w and (b) the horizontal velocity u through a density interface *vs.* the vertical co-ordinate ξ . The Richardson number (based on the density difference across the interface, the integral length scale and the r.m.s. turbulent velocity near the interface) was 280. The centre and the edge of the interface are shown by arrows on the ordinate.

intensity of the laser light through the rotating diffraction grating. The diameter (to the e^{-2} intensity levels) of the probe volume was estimated to be $360 \mu\text{m}$, which corresponded to 70 fringes. (This was estimated by shining the beams through a microscope objective lens and viewing the image of the fringe planes on a distant screen.) The lens and pinhole combination in front of the photomultiplier was arranged such that light was received from only the central 60 fringes. Any movement of the laser beams will cause an irregular amplitude modulation on the signal from the photomultiplier. The laser beams were arranged to pass through the turbulent region of the forced plume and in the experiment of figure 6(b) the amplitude modulation of the sine wave was not noticeably affected. The movement of the laser beams must have been less than $60 \mu\text{m}$ at the probe volume.

The method of this paper has been used to take velocity measurements in a mixed layer which was entraining fluid across a density interface and also to obtain vertical and horizontal velocity measurements through a density interface. These measurements will be reported elsewhere (McDougall 1979) but we note that at no time did we encounter any extra difficulties because we were working with a stratified fluid. Figure 7 shows an example of measurements of the horizontal and vertical root-mean-square velocities through a density interface between two well-mixed turbulent layers. The density difference across the interface was 0.015 g/ml , and if this density difference had been simply due to different concentrations of common salt, the two laser beams would have moved about laterally through several millimetres and any velocity measurements would have been impossible.

At no stage in any of the experiments were any salt fingers observed. If salt fingers had been present then they would have been visible because the different diffusivities of the two solutes would have transported the solutes unevenly in a manner similar to that discussed in §4. This can readily be observed by using common salt instead of Epsom salts. Fingers can then be clearly seen, even though the two initial solutions have the same refractive index. This is because the condition of Huppert & Manins (1973) is not fulfilled by the combination of common salt and sugar.

6. Wander of a laser beam

In this section we attempt to describe quantitatively the wander of a laser beam as it advances through a turbulent medium. We consider homogeneous isotropic turbulence in which variations in refractive index are caused by the concentration θ of a passive scalar. By evaluating the typical spatial gradients of the refractive index which occur in this idealized turbulent flow, we obtain an estimate of the typical root-mean-square lateral deviation of a laser beam.

Consider a laser beam propagating in the $+x$ direction. The beam will be made to deviate from a straight-line path by inhomogeneities in the refractive index. The deviation (or wander) in the x, y plane is caused by spatial gradients of the refractive index in the y direction; similarly, the wander in the x, z plane is caused by spatial gradients of the refractive index in the z direction. Let us first consider only the effect of the gradients of the refractive index in the y direction (i.e. $\partial n/\partial y$). If ϕ is the angle (assumed small) which the beam makes with the x axis, then to first order we have (Mowbray 1967)

$$\frac{d\phi}{dx} = \frac{1}{n} \frac{\partial n}{\partial y} \equiv \frac{1}{n} \frac{\partial}{\partial y} (n - n_0). \quad (15)$$

The increase in refractive index over that of pure water (n_0) is assumed to be proportional to the scalar concentration θ , i.e. $n - n_0 = b\theta$, where b is a constant, so

$$\frac{d\phi}{dx} = \frac{b}{n} \frac{\partial \theta}{\partial y}. \quad (16)$$

The displacement s in the y direction after passing through a length A of the turbulent environment is

$$s = \int_0^A \phi(x) dx = \frac{b}{n_0} \int_0^A \int_0^x \frac{\partial \theta}{\partial y} dx' dx \quad (17)$$

[where we have made the approximation of replacing n in the denominator of (16) by n_0], and the quantity of interest to us is $(s^2)^{\frac{1}{2}}$, i.e. the root-mean-square wander of the laser beam in the y direction.

For dissolved salts in water, where the Schmidt number ($= \nu/D$, where D is the diffusivity of the scalar quantity) is large, the largest spatial concentration gradients occur in the 'convective-viscous' wavenumber range of the concentration spectrum. In this high wavenumber range the three-dimensional concentration spectrum is given by (Batchelor 1959)

$$\Phi_{\theta\theta}(\mathbf{k}) = \frac{1}{4\pi} C'_\theta \epsilon_\theta \left(\frac{\nu}{\epsilon}\right)^{\frac{1}{2}} k^{-3}, \quad (18)$$

where $C'_\theta = \text{constant} \approx 2$ (Townsend 1976, p. 347),

$$\epsilon_\theta = \overline{\theta^2 (\overline{q^2})^{\frac{1}{2}}} / L_\theta, \quad \epsilon = \frac{1}{3} \overline{(q^2)^{\frac{1}{2}}} / L,$$

L = integral length scale of the turbulent velocity field,

L_θ = length scale of the scalar field ($L_\theta \approx L$),

$$\overline{q^2} = \overline{u_1^2 + u_2^2 + u_3^2}, \text{ where the velocity vector } \mathbf{u} = (u_1, u_2, u_3),$$

k = magnitude of the wavenumber vector $\mathbf{k} = (k_1, k_2, k_3)$,

ν = kinematic viscosity,

θ = concentration of the scalar property.

The three-dimensional spectrum of $\partial\theta/\partial y$ in this wavenumber range is then $k_2^2 \Phi_{\theta\theta}(\mathbf{k})$ and we shall call this $\Psi(\mathbf{k})$.

Now, from our knowledge of the statistics of a double integral (see, for example, Tennekes & Lumley 1972, equation 6.5.16) we have

$$\overline{s^2} = \frac{2b^2}{3n_0^2} A^3 \int_0^A \overline{\frac{\partial\theta}{\partial y}(x+x', y, z) \frac{\partial\theta}{\partial y}(x, y, z)} dx'. \quad (19)$$

Since A is much greater than the length scale over which $\partial\theta/\partial y$ remains correlated with itself, the value of the integral will not be substantially changed by replacing the upper limit of integration with infinity. The correlation function

$$\overline{\frac{\partial\theta}{\partial y}(x+x', y, z) \frac{\partial\theta}{\partial y}(x, y, z)}$$

is related to the one-dimensional spectrum function of $\partial\theta/\partial y$ by

$$\Psi(k_1) = \frac{1}{2\pi} \int_{-\infty}^{\infty} \exp(-ik_1 x') \overline{\frac{\partial\theta}{\partial y}(x+x', y, z) \frac{\partial\theta}{\partial y}(x, y, z)} dx', \quad (20)$$

where

$$\Psi(k_1) = \int_{-\infty}^{\infty} \int_{-\infty}^{\infty} \Psi(\mathbf{k}) dk_2 dk_3. \quad (21)$$

From (20) we see that $\pi\Psi(k_1 = 0)$ is equal to the integral in (19), so we proceed to evaluate $\Psi(k_1)$ from (21). The convective-viscous wavenumber range ends near $k = k'_c = (\nu/D)^{\frac{1}{2}} \epsilon^{\frac{1}{2}} \nu^{-\frac{1}{2}}$ (see equation 8.5.11 of Townsend 1976) so we assume that the integration in (21) terminates at $k_2^2 + k_3^2 = k'_c{}^2$. We then have

$$\begin{aligned} \Psi(k_1) &= \frac{1}{4\pi} C'_\theta \epsilon_\theta \left(\frac{\nu}{\epsilon}\right)^{\frac{1}{2}} \int_0^{2\pi} \int_0^{k'_c} \frac{k^2 \cos^2 \gamma}{(k_1^2 + k^2)^{\frac{3}{2}}} k dk d\gamma \\ &= \frac{1}{4\pi} C'_\theta \epsilon_\theta \left(\frac{\nu}{\epsilon}\right)^{\frac{1}{2}} \pi \left\{ 2(k_1^2 + k'_c{}^2)^{\frac{1}{2}} - 2k_1 - \frac{k'_c{}^2}{(k_1^2 + k'_c{}^2)^{\frac{1}{2}}} \right\}, \end{aligned}$$

so $\Psi(k_1 = 0) = \frac{1}{4} C'_\theta \epsilon_\theta (\nu/\epsilon)^{\frac{1}{2}} k'_c$. This leads to the following equation for $(\overline{s^2})^{\frac{1}{2}}$:

$$(\overline{s^2})^{\frac{1}{2}} = \left(\frac{\pi}{6}\right)^{\frac{1}{2}} \frac{b}{n_0} C'_\theta{}^{\frac{1}{2}} \epsilon_\theta^{\frac{1}{2}} \left(\frac{\nu}{\epsilon}\right)^{\frac{1}{4}} A^{\frac{3}{2}} k'_c{}^{\frac{1}{2}}. \quad (22)$$

The most important point which we wish to emphasize here is that the typical lateral displacement in the y direction [as estimated by (22)] is proportional to $\epsilon_\theta^{\frac{1}{2}}$, which is in turn proportional to $[(n - n_0)^2]^{\frac{1}{2}}$. In laser-Doppler anemometry we have two laser beams which wander independently in both the y and the z direction. A signal is received by the anemometer only when *both* laser beams pass simultaneously through the small region from which light is collected by the photo-detector (the probe volume). Consider the situation of figure 6(a), where the laser beams were observed to move about by up to 5 mm. We estimate the r.m.s. lateral deviation to be one-quarter of this, i.e. 1.25 mm. Figure 8 shows a Gaussian probability density function (p.d.f.) with this standard deviation; the extent of the probe-volume diameter of 360 μm is also shown. The shaded area of this graph is 0.114 of the total area under the Gaussian curve. The proportion of time during which both beams pass through the probe volume is then given by $(0.114)^4 = 0.00017$. This fourth-power dependence is due to the fact that both laser beams wander independently in the y and z directions.

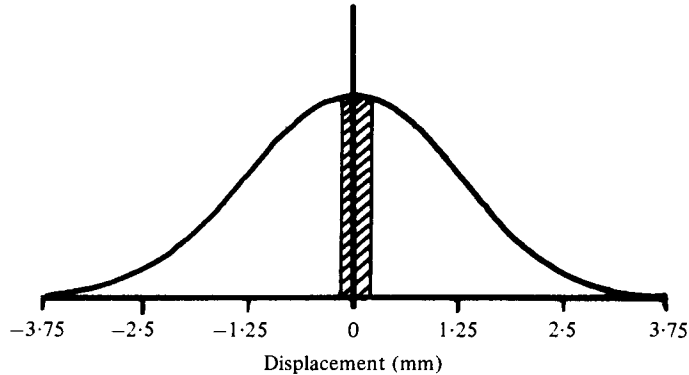


FIGURE 8. Gaussian probability density function with a standard deviation of 1.25 mm. The probe volume is $360\ \mu\text{m}$ in diameter and is shown as the shaded area in the figure.

The difference in refractive index between the two solutions in figure 6(a) was 57×10^{-4} , but when the method of this paper is used to match the refractive indices, the difference in refractive index between the two solutions will be 2×10^{-4} at most. This means that $(\overline{s^2})^{\frac{1}{2}}$ will be reduced by a factor of $\frac{5.7}{2}$ (because $(\overline{s^2})^{\frac{1}{2}} \propto \epsilon_b^{\frac{1}{2}} \propto [(n - n_0)^2]^{\frac{1}{2}}$). The r.m.s. lateral deviation is then expected to be $\frac{2}{5.7} \times 1.25\ \text{mm} = 44\ \mu\text{m}$. This small beam movement means that the beams will not wander outside the probe volume and so will always cross in the probe volume. The random superimposed frequency shifts will also be quite small and could normally be neglected.

In summary, this treatment of laser-beam wander shows that the r.m.s. lateral deviation is proportional to $[(n - n_0)^2]^{\frac{1}{2}}$, and together with the fourth-power dependence on the relative areas of figure 8, this theoretical model shows why the method of this paper is so successful.

The estimated values of the parameters for the experiment of figure 6(a) are $(\overline{q^2})^{\frac{1}{2}} = 5\ \text{cm s}^{-1}$, $A = 2\ \text{cm}$, $C'_\theta = 2$, $\nu = 0.01\ \text{cm}^2\ \text{s}^{-1}$, $L = L_\theta = 0.5\ \text{cm}$, $\theta^2 = \frac{1}{5}(0.03)^2$, $b = 0.2$ and $D = 0.61 \times 10^{-5}\ \text{cm}^2\ \text{s}^{-1}$. Inserting these in (22) gives $(\overline{s^2})^{\frac{1}{2}} = 2\ \text{mm}$. This is the correct order of magnitude for the standard deviation of the lateral displacement (in keeping with the observed maximum displacement of $\pm 5\ \text{mm}$) but is probably too high by a factor of two.

We note in passing that the variations in refractive index in gases (and in flames in particular) are remarkably small compared with those that commonly occur in stratified *liquids*. The refractive index of air, for example, changes by only 2×10^{-4} when its temperature is raised by $1000\ ^\circ\text{C}$ (Weast 1971). The same change in refractive index of a solution of common salt occurs at a density difference of only $0.0007\ \text{g/ml}$, i.e. a relative density difference of $0.07\ \%$. Consequently many laser-Doppler anemometer studies of flames have been reported (e.g. Durão & Whitelaw 1974).

I am grateful to Dr A. A. Townsend and Professor W. H. Munk for valuable discussions after which the ideas in §6 evolved. This work was begun at the University of Cambridge, where financial support was provided by a George Murray Overseas Scholarship (given by the University of Adelaide), and was completed at the Australian National University, where I have been supported by a Queen's Fellowship in Marine Science.

REFERENCES

- BATCHELOR, G. K. 1959 Small-scale variation of convected quantities like temperature in a turbulent fluid. Part I. *J. Fluid Mech.* **5**, 113–133.
- CARLOS, C. R. & RICHARDSON, J. F. 1967 Particle seed distributions in a fluidised system. *Chem. Engng Sci.* **22**, 705–706.
- DURÃO, D. F. G. & WHITELAW, J. H. 1974 Instantaneous velocity and temperature measurements in oscillating diffusion flames. *Proc. Roy. Soc. A* **338**, 479–501.
- HUPPERT, H. E. & MANINS, P. C. 1973 Limiting conditions for salt-fingering at an interface. *Deep-Sea Res.* **20**, 315–323.
- MCDUGALL, T. J. 1979 Measurements of turbulence in a zero-mean-shear mixed layer. *J. Fluid Mech.* (In press).
- MOWBRAY, D. E. 1967 The use of schlieren and shadowgraph techniques in the study of flow patterns in density stratified liquids. *J. Fluid Mech.* **27**, 595.
- SHIRTCLIFFE, T. G. L. 1973 Transport and profile measurements of the diffusive interface in double diffusive convection with similar diffusivities. *J. Fluid Mech.* **57**, 27–43.
- TENNEKES, H. & LUMLEY, J. L. 1972 *A First Course in Turbulence*. M.I.T. Press.
- TOWNSEND, A. A. 1976 *The Structure of Turbulent Shear Flow*, 2nd edn. Cambridge University Press.
- TURNER, J. S. 1973 *Buoyancy Effects in Fluids*. Cambridge University Press.
- WASHBURN, E. W. (ed.) 1927 *The International Critical Tables*, vol. III. McGraw-Hill.
- WEAST, R. C. (ed.) 1971 *Handbook of Chemistry and Physics*, 52nd edn. Chemical Rubber Co.

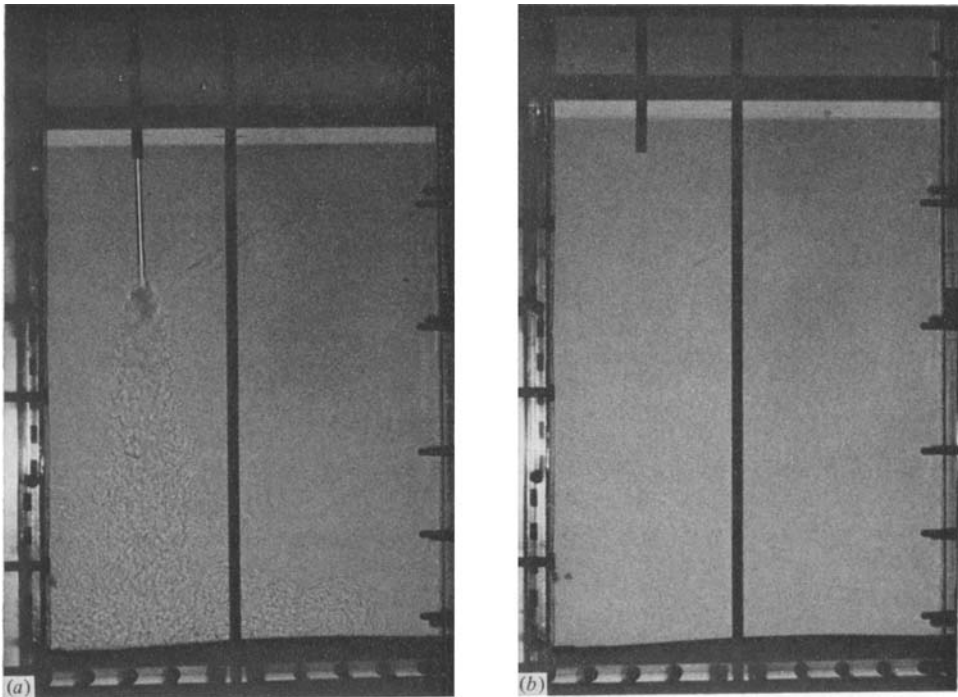


FIGURE 6. Shadowgraphs of a forced plume of Epsom-salts solution. (a) Epsom-salts solution entering a tank of fresh water. Note the long region of laminar flow between the pipe exit and the breakdown to turbulence. (b) Epsom-salts solution entering a tank of sugar solution of the same refractive index; no shadowgraph can be seen. The density difference between the plume and the tank fluid was the same in both cases.